A new LDPC decoding scheme for PDM-8QAM BICM coherent optical communication system*

LIU Yi (刘怡)[1], **ZHANG Wen-bo** (张文博)[2]**, **XI Li-xia** (席丽霞)[1], **TANG Xian-feng** (唐先锋)[1], and **ZHANG Xiao-guang** (张晓光)[1]

1. State Key Laboratory of Information Photonics and Optical Communications, Beijing University of Posts and Telecommunications, Beijing 100876, China

2. School of Science, Beijing University of Posts and Telecommunications, Beijing 100876, China

(Received 25 September 2015; Revised 15 October 2015)

A new log-likelihood ratio (LLR) message estimation method is proposed for polarization-division multiplexing eight quadrature amplitude modulation (PDM-8QAM) bit-interleaved coded modulation (BICM) optical communication system. The formulation of the posterior probability is theoretically analyzed, and the way to reduce the pre-decoding bit error rate (*BER*) of the low density parity check (LDPC) decoder for PDM-8QAM constellations is presented. Simulation results show that it outperforms the traditional scheme, i.e., the new post-decoding *BER* is decreased down to 50% of that of the traditional post-decoding algorithm.

Document code: A **Article ID:** 1673-1905(2015)06-0449-4

DOI 10.1007/s11801-015-5182-z

By increasing the symbol rate, the number of carriers and using high-order modulation, the channel capacity can be improved significantly. For instance, 400 Gbit wavelength division multiplexing (WDM) system can be realized by using polarization-division multiplexing quadrature phase shift keying (PDM-QPSK) system[1] or polarization-division multiplexing sixteen quadrature amplitude modulation (PDM-16QAM) system[2]. Unfortunately, nonlinear effects will greatly reduce the transmission distance when higher-order QAM is used. PDM-8QAM is thought to be a trade-off between transmission distance and system capacity, which has been tested in long-haul optical communication system[3-5].

Forward error correction (FEC) technology with high coding gain and high bit error rate (*BER*) threshold is one of the key enabling technologies for next generation high-speed long-haul optical fiber communications. Low density parity check (LDPC) code has been introduced to improve system tolerance to the fiber channel impairment[6,7], where the posterior probability calculation is the crucial part in the LDPC decoding module[8]. Unlike the regular *M*-ary quadrature amplitude modulation (*M*-QAM) format, such as QPSK and 16-QAM, whose constellations are on the squared grid, the decision regions of 8-QAM for calculating posterior probability are not regular rectangle. Therefore, the log-likelihood ratio (LLR) message estimation could be wrong at the edges of these irregular decision regions, which greatly influences the correction of decoding signals.

Bit-interleaved coded modulation (BICM) was firstly introduced by Zehavi in 1992. The combination of BICM system and high-order modulation has become a hot topic recently[9,10], due to its advantages in the anti-noise performance. In this paper, we propose a new posterior probability calculation method for BICM PDM-8QAM system to lower the pre-decoding *BER* and therefore lower the post-decoding *BER*.

The schematic diagram of a typical BICM system is shown in Fig.1. A binary information vector $\boldsymbol{x}=[x_1, x_2, \ldots, x_{N-M}]$ is encoded by quasi-cyclic LDPC (QC-LDPC) method, and let $\boldsymbol{u}=[u_1, u_2, \ldots, u_N]$ be the output of the QC-LDPC encoder. The code rate can be calculated by $R=1-M/N$, where N and M are the lengths of QC-LDPC code and parity check nodes, respectively. To improve the tolerance of noise, the QC-LDPC code $\boldsymbol{u}$ is fed into an interleaver. To facilitate the gray mapping, the output of interleaver needs to be parallelized by a serial to parallel transformer before the transmission in optical channel. The output of serial to parallel transformer is represented by matrix $\boldsymbol{c}$ as

$$\boldsymbol{c}=\begin{bmatrix} c_{1,1} & c_{1,2} & \cdots & c_{1,k} \\ c_{2,1} & c_{2,2} & \cdots & c_{2,k} \\ \vdots & \vdots & \ddots & \vdots \\ c_{N/k,1} & c_{N/k,2} & \cdots & c_{N/k,k} \end{bmatrix}_{(N/k)*k}=\begin{bmatrix} \boldsymbol{c}_1 \\ \boldsymbol{c}_2 \\ \vdots \\ \boldsymbol{c}_{N/k} \end{bmatrix}_{N/k}. \tag{1}$$

* This work has been supported by the National Natural Science Foundation of China (No.61205065), the Fund of State Key Laboratory of Information Photonics and Optical Communications and the Fundamental Research Funds for the Central Universities in China (No.2014RC1201).

** E-mail: zhangwb@bupt.edu.cn

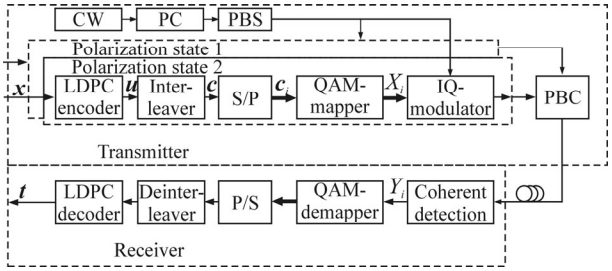

CW: continuous wave laser; PC: polarization controller; PBS: polarization beam splitter; S/P: serial to parallel transformer; P/S: parallel to serial transformer; PBC: polarization beam combiner

Fig.1 Schematic diagram of a typical BICM system

By gray mapping, $\boldsymbol{c}_i$ can be mapped into a symbol X_i, where i={1, 2, …, N/k}. In case of 8-QAM mapping, where k=log$_2$8=3, the mapping function is defined as μ: S_m=μ(b), which can associate a 3-bit sequence b=[b_1, b_2, b_3] with a complex value S_m according to signal constellation rule. As in Ref.[11], the constellation map is shown in Fig.2, and the mapping function μ is given in Tab.1.

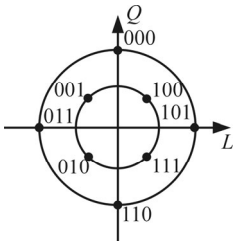

Fig.2 8-QAM constellation diagram

Tab.1 8-QAM mapping rules

b=[b_1, b_2, b_3]	$S_m(I_m, Q_m)$
000	$(0, 1+\sqrt{3})$
001	$(-1, 1)$
011	$(-1-\sqrt{3}, 0)$
010	$(-1, -1)$
110	$(0, -1-\sqrt{3})$
111	$(1, -1)$
101	$(1+\sqrt{3}, 0)$
100	$(1, 1)$

At the receiver end, the received symbol Y_i can be obtained by the coherent detector. An inverse mapping based on LLR is involved. By using this inverse mapping, Y_i is demapped into a 3-bit sequence y_i=[$y_{i,1}$, $y_{i,2}$, $y_{i,3}$], where i∈ {1, 2, 3, …, N/3}.

Based on the following theory, the inverse mapping is defined. Let Y be the symbol before transmission and $\hat{Y}$ be the symbol obtained by coherent detector. The posterior probability of Y can be calculated by Bayes law as[12,13]

$$P_m = \frac{1}{W}\Pr\left\{\hat{Y}\middle|Y=S_m\right\} = \frac{1}{\sqrt{2\pi}\sigma}\exp\left(-\frac{\left|\hat{Y}-S_m\right|}{2\sigma^2}\right). \quad (2)$$

The idea to define the inverse mapping is to calculate posterior probability P_m of every S_m with respect to $\hat{Y}$ as shown in Fig.3(a), then calculate LLR to make judgment, and finally $\hat{Y}$ can be associated with the 3-bit sequence y_i.

Notice that each symbol S_m is associated with a 3-bit sequence b=[b_1, b_2, b_3], so all symbols can be classified into two categories according to the value of b_j (j=1,2,3) as {S_m, b_j=1} and {S_m, b_j=0}. Thus the initialization message of bit $y_{i,j}$ can be defined as

$$q^0_{ij}(1) = \Pr\left\{y_{i,j}=1\middle|\hat{Y}\right\} = \sum_{m\in\{S_m, b_j=1\}}\Pr\left\{Y=S_m\middle|\hat{Y}\right\} = \sum_{m\in\{S_m, b_j=1\}}P_m, \quad (3)$$

$$q^0_{ij}(0) = \Pr\left\{y_{i,j}=0\middle|\hat{Y}\right\} = \sum_{m\in\{S_m, b_j=0\}}\Pr\left\{Y=S_m\middle|\hat{Y}\right\} = \sum_{m\in\{S_m, b_j=0\}}P_m, \quad (4)$$

and the LLR message can be calculated by

$$L\left(y_{i,j}\middle|\hat{Y}\right) = \log_2\frac{\Pr\left\{y_{i,j}=1\middle|\hat{Y}\right\}}{\Pr\left\{y_{i,j}=0\middle|\hat{Y}\right\}} = \frac{q^0_{ij}(1)}{q^0_{ij}(0)} = \frac{\sum_{m\in\{S_m, b_j=1\}}P_m}{\sum_{m\in\{S_m, b_j=0\}}P_m}. \quad (5)$$

So the pre-decoding sequence y_i=[$y_{i,1}$, $y_{i,2}$, $y_{i,3}$], i∈ {1, 2, 3, …, N/3} can be obtained by

$$y_{i,j} = \begin{cases} 1, L\left(y_{i,j}\middle|\hat{Y}\right) > 1 \\ 0, 0 < L\left(y_{i,j}\middle|\hat{Y}\right) < 1 \end{cases}. \quad (6)$$

In Fig.3, we show the decision region of Eq.(6) together with constellation map. Fig.3(a) shows the ideal Voronoi diagram[14] for 8-QAM gray mapping. In Fig.3(b)−(d), the black regions show the decision regions for $y_{i,1}$=1, $y_{i,2}$=1, $y_{i,3}$=1, respectively. If $\hat{Y}$ falls into the black region, the corresponding bit $y_{i,j}$ is judged as "1".

According to Eq.(5), both the mapping function μ and the method to calculate P_m will affect the shape of decision region. As shown in Fig.3(b), we can see that there are some differences between the real decision region and ideal Voronoi diagram for $y_{i,1}$=1 and $y_{i,1}$=0 at the edges. Error type I means that $y_{i,1}$ should be judged as "1", but it is judged as "0", and error type II means that $y_{i,1}$ should be judged as "0", but it is judged as "1". It is clear that all types of errors will increase the *BER*. Similar analyses also can be used for Fig.3(c) and (d). In this paper, we suggest a new method to define P_m, so that the difference between decision region and ideal Voronoi diagram can be significantly decreased, and the pre-decoding *BER* performance can also be improved.

It is easy to conclude from Eq.(2) that $P_m \propto |\hat{Y}-S_m|^{-1}$, which means the closer $\hat{Y}$ to S_m, the bigger P_m is. As shown in Fig.3(b)—(d), $|L(y_{i,j}|\hat{Y})-1|$ at the edge of two

neighboring regions is very close to "0", so it is easy to be misjudged. To decrease the misjudgment, we increase the absolute value $|L(y_{i,j}|\ \hat{Y}\ )-1|$ by changing P_m to $P_{m2}=P_m^{\ 2}$. To be convenient, we set the traditional form P_m as P_{m1}. Fig.4 shows the decision regions of P_{m1} and P_{m2} at $y_{i,1}$.

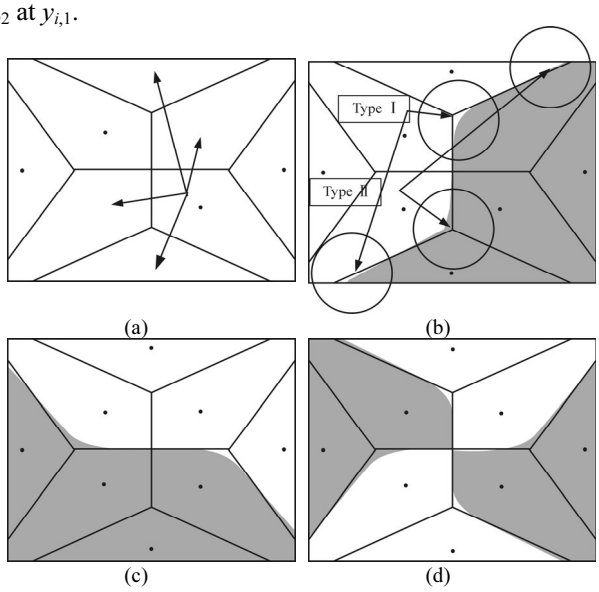

Fig.3 (a) The ideal Voronoi diagram for 8-QAM gray mapping; Voronoi diagrams with black regions representing the decision regions for (b) $y_{i,1}$=1, (c) $y_{i,2}$=1 and (d) $y_{i,3}$=1, respectively

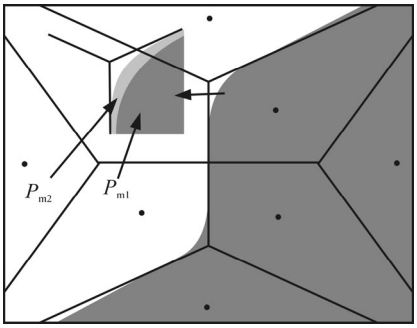

Fig.4 Comparison between the decision regions of P_{m1} and P_{m2} at $y_{i,1}$

As shown in Fig.4, compared with the decision region of the traditional form of P_{m1}, that of P_{m2} leaves smaller blanket area at the edge of the neighboring region, which leads to better pre-decoding *BER* performance. As we know, the decrease of pre-decoding *BER* results in the decrease of post-decoding *BER*. To test the post-decoding *BER* performance of P_{m1} and P_{m2}, we apply LLR belief propagation (LLR-BP) based min-sum algorithm[15,16] and QC-LDPC codes to the BICM PDM-8QAM system. The decoding process is clarified in Fig.5.

The output sequence $\boldsymbol{t}$ from the LDPC decoder is obtained by $L^{(f)}(q_m)$ after decoding iterations. During f times of iterations, the message transferred from the check nodes to variable nodes is given as

$$L^{(f)}\left(r_{mn}\right)= \prod_{m\in Check_n} \operatorname{sgn}\left[L^{(f-1)}\left(q_m\right)\right] * \min_{m\in Check_n}\left[\left|L^{(f-1)}\left(q_m\right)\right|\right] \quad , \tag{7}$$

where $check_n$ is a set of check nodes connected with variable nodes. The message transferred from the variable nodes to check n nodes is written as

$$L^{(f)}\left(q_m\right)=L\left(y_{i,j}\left|\hat{Y}\right.\right)+\sum_{n\in Variable_m} L^{(f)}\left(r_{mn}\right), \tag{8}$$

where $variable_m$ is a set of variable nodes connected with check nodes m. The maximum iteration time is set to be *maxiter*.

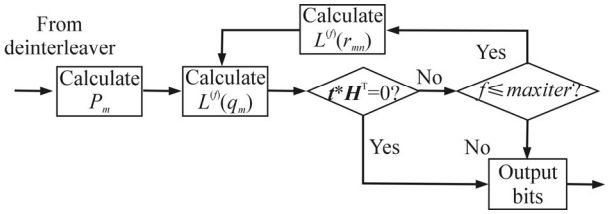

Fig.5 Schematic diagram of LDPC decoding process

To test the performance of the proposed calculation method, we set up the BICM 8QAM system as shown in Fig.1. The maximum iteration time of the LDPC decoder is set to be 5, 10 and 15, respectively.

We apply QC-LDPC codes as the check matrix of the LDPC encoder. Compared with the standard randomly constructed LDPC codes, QC-LDPC check matrix is encoded with shift register that requires less amount of flash memory, which can significantly decrease the circuit complexity[17,18].

The parity check matrix ($\boldsymbol{H}$) of a QC-LDPC code could be shown by an array of sub-matrices as follows

$$\boldsymbol{H}_{\mathrm{qc}}=\begin{pmatrix} \boldsymbol{A}_{1,1} & \cdots & \boldsymbol{A}_{1,N} \\ \vdots & \ddots & \vdots \\ \boldsymbol{A}_{M,1} & \cdots & \boldsymbol{A}_{M,N} \end{pmatrix}. \tag{9}$$

Each sub-matrix $\boldsymbol{A}_{m,n}$ with $m\in\{1, 2, \ldots, M\}$ and $n\in\{1, 2, \ldots, N\}$ is a circular matrix. We design a 20% over-head (OH) QC-LDPC code with column weight of 3 and row weight of 15. The first row of each sub-matrix is a vector which contains only "1" in the fth position, while other rows are the permutation of the first row. We set the size of the sub-matrix as 1 123×1 123. Thus the total size of the parity check matrix is 3 369×16 845.

We define parameter $\hat{a}$ as the ratio of the *BER* of the proposed posterior probability form P_{m2} to that of the original posterior form P_{m1}, which can be expressed as

$$\hat{a}=\frac{BER(P_{m2})}{BER(P_{m1})}. \tag{10}$$

The four lines in Fig.6(a) show $\hat{a}$ representing the pre-decoding *BER* ratio and the post-decoding *BER* ratios for 3 different iteration times, respectively. As the signal-to-noise ratio (*SNR*) goes from 0 dB to 5 dB, $\hat{a}$ as the pre-decoding *BER* ratio remains a steady level at about 0.96, while the $\hat{a}$ values as the post-decoding *BER* ratios for 3

different iteration times all fall down rapidly. This means that the decrease of the pre-decoding *BER* ratio can significantly decrease the post-decoding *BER* ratio. For high *SNR*, $\hat{a}$ can be reduced to 0.5.

From Fig.6(b), we can see that the *SNR* for a fixed *BER* of the new form of P_{m2} outperforms that of the traditional form of P_{m1} by 0.2 dB at post-decoding *BER* of 10^{-5}. As the maximum iteration time increases, the effect is obvious. Besides, this method can be applied to universal LDPC decoder without increasing the circuit complexity.

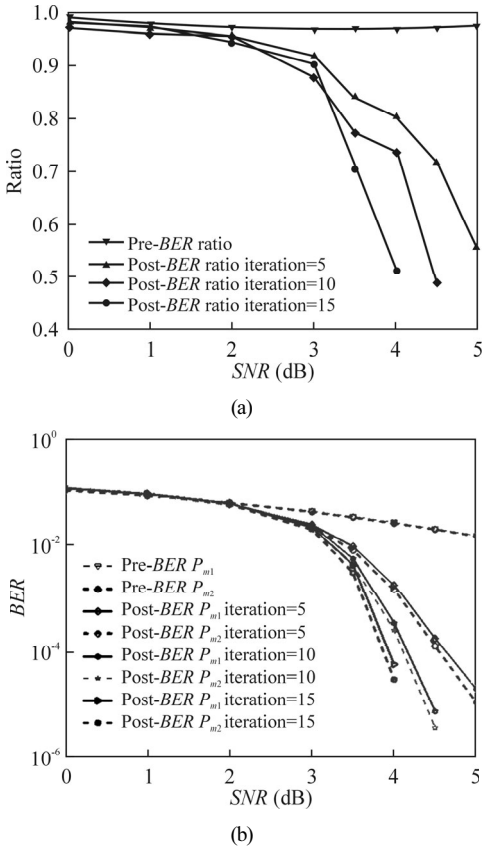

Fig.6 (a) Pre-decoding *BER* (pre-*BER*) ratio and post-decoding *BER* (post-*BER*) ratio for 3 different iteration times versus *SNR*; (b) Pre-*BER* ratio and post-*BER* ratio for 3 different iteration times with two forms of P_{m1} and P_{m2} versus *SNR*

We propose a new method to calculate the posterior probability, which can reduce the pre-decoding *BER* and post-decoding *BER* of LDPC decoder in BICM-ID PM-8QAM system. Theoretical analysis of the method is discussed. Simulation results show that the new form outperforms the traditional form by 0.2 dB when *BER* equals 10^{-5}, and $\hat{a}$ decreases to 50%. Moreover, this method can reach a lower error floor as the increase of *SNR*.

References

[1] Junwen Zhang, Jianjun Yu, Zhensheng Jia and Hung-Chang Chien, Journal of Lightwave Technology **32**, 3239 (2014).

[2] V. V. Sleiffer, D. van den Borne, V. Veljanovski, M. Kuschnerov, M. Hirano, Y. Yamamoto, T. Sasaki, S. L. Jansen and H. Waardt, Transmission of 448-Gb/s Dual-Carrier POLMUX-16QAM over 1230 km with 5 Flexi-Grid ROADM Passes, Optical Fiber Communication Conference, 2012.

[3] X. Zhou, J. Yu, M. Huang, Y. Shao, T. Wang, P. Magill, M. Cvijetic, L. Nelson, M. Birk, G. Zhang, S. Ten, H. Matthew and S. Mishra, 32Tb/s (320×114Gb/s) PDM-RZ-8QAM Transmission over 580 km of SMF-28 Ultra-Low-Loss Fiber, Conference on Optical Fiber Communication, 1 (2009).

[4] I. Djordjevic and B. Vasic, Journal of Lightwave Technology **24**, 420 (2006).

[5] Infinerab Corporation, Infinera Demos PM-8QAM cross Telstra Submarine Cable, http://www.fibre-systems.com/news/story/infinera-demos-pm-8qam-across-telstra-submarine-cabl, 2015.

[6] I. B. Djordjevic and T. Wang, On the LDPC-Coded Modulation for Ultra-High-Speed Optical Transport in the Presence of Phase Noise, Optical Fiber Communication Conference and Exposition and the National Fiber Optic Engineers Conference, 1 (2013).

[7] YUAN Jian-guo, TONG Qing-zhen, HUANG Sheng and WANG Yong, Optoelectronics Letters **9**, 469 (2013).

[8] T. Koike-Akino, D. Millar, K. Kojima and K. Parsons, Coded Modulation Design for Finite-Iteration Decoding and High-Dimensional Modulation, Optical Fiber Communications Conference and Exposition, 1 (2015).

[9] J. Zhang, H. Chien, Z. Dong and J. Xiao, Transmission of 480-Gb/s Dual-carrier PM-8QAM over 2550 km SMF-28 Using Adaptive Pre-equalization, Optical Fiber Communications Conference and Exposition, 1 (2014).

[10] Sha Li, Chongxiu Yu, Zhe Kang, Gerald Farrell and Qiang Wu, Chinese Optics Letters **12**, 010604 (2014).

[11] TAO Jin-jing, ZHANG Yang-an, HUANG Yong-qing, ZHANG Jin-nan, YUAN Xue-guang and LI Yu-peng, Optoelectronics Letters **9**, 132 (2013).

[12] S. Ten Brink, J. Speidel and Ran-Hong Yan, Iterative Demapping and Decoding for Multilevel Modulation, Global Telecommunications Conference **1**, 579 (1998).

[13] S. Ten Brink, G. Kramer and A. Ashikhmin, IEEE Transactions on Communications **52**, 670 (2004).

[14] G. Como and F. Fagnani, Society for Industrial and Applied Mathematics (SIAM) Journal of Discrete Mathematics **23**, 19 (2008).

[15] R. G. Gallager, IEEE Transactions on Information Theory **8**, 21 (1962).

[16] R. M. Tanner, IEEE Transactions on Information Theory **27**, 533 (1981).

[17] Deyuan Chang, Fan Yu, Zhiyu Xiao, Yang Li, Stojanovic N., Changsong Xie, Xiaozhong Shi, Xiaogeng Xu and Qianjin Xiong, FPGA Verification of a Single QC-LDPC Code for 100 Gb/s Optical Systems without Error Floor down to BER of 10^{-15}, Optical Fiber Communication Conference and Exposition and National Fiber Optic Engineers Conference, 1 (2011).

[18] M. P. C. Fossorier, IEEE Transactions on Information Theory **50**, 1788 (2004).